Journal of the Korean Nuclear Society
Volume 27, Number 3, June 1995

Natural Convection in a Water Tank with a Heated Horizontal Plate Facing Downward

Sun Kyu Yang and Moon Ki Chung
Korea Atomic Energy Research Institute

Helmut Hoffmann
Kernforschungszentrum Karlsruhe/IATF, Germany
(Received October 28, 1994)

아래로 향한 수평가열판이 있는 수조에서의 자연대류

양선규 · 정문기
한국원자력연구소

Helmut Hoffmann
KfK/IATF, 독일
(1994. 10. 28 접수)

Abstract

Experimental and computational studies were carried out to investigate the natural convection of the single phase flow in a tank with a heated horizontal plate facing downward. This is a simplified model for investigations of the influence of a core melt at the bottom of a reactor vessel on the thermal hydraulic behavior in a water filled cavity surrounding the vessel. In this case the vessel is simulated by a hexahedron insulated box with a heated plate horizontally mounted at the bottom of the box. The box with the heated plate is installed in a water filled hexahedron tank. Coolers are immersed in the U-type water volume between the box and the tank. Although the multicomponent flows exist more probably below the heated plate in reality, present study concentrates on the single phase flow in a first step prior to investigating the complicated multicomponent thermal hydraulic phenomena. In the present study, in order to get a better understanding for the natural convection characteristics below the heated plate, the velocity and temperature are measured by LDA(Laser Doppler Anemometry) and thermocouples, respectively. And flow fields are visualized by taking pictures of the flow region with suspended particles. The results show the occurrence of a very effective circulation of the fluid in the whole flow area as the heater and coolers are put into operation. In the remote region below the heated plate the flow is nearly stagnant, and a remarkable temperature stratification can be observed with very thin thermal boundary. Analytical predictions using the FLUTAN code show a reasonable matching of the measured velocity fields.

요 약

아래를 향한 가열 수평 평판이 있는 수조에서의 자연대류 현상을 규명하기 위한 실험적, 해석적인 연구를 수행하였다. 이는 압력용기 하부에 용융물이 있을때 캐비티내에서의 열수력현상을 규명하기 위한 간단화된 모델에 관한 연구이다. 압력 용기는 하부에 가열평판이 부착된 직육면체 단열 상자로 모의하고 이 상자는 물이 차 있는 수조에 설치된다. 냉각기는 정상상태의 유동 조건을 만들기 위해 상자와 수조사이의 U자 형태의 유동 영역에 설치된다. 실제 압력용기 하부에서는 다상 유동이 발생할 확율이 크나 본 연구는 복잡한 다상 유동의 열수력 현상을 규명하기 위한 첫 단계 시도로서 단상유체를 사용한 실험 및 해석연구이다. 본 연구에서는 가열 평판 아래에서의 자연대류현상특성을 더욱 잘 이해하기 위해 LDV와 열전대를 사용하여 속도와 온도를 측정하였다. 또한 입자가 부상된 유동장을 사진 찍어 유동을 가시화하였다. 실험결과는 다음과 같다. 유체는 가열판과 냉각기가 작동할 때 매우 효과적으로 전 유동장에 걸쳐 순환한다. 가열판 하부에서 유동이 정체된 영역이 있고 매우 얇은 열 경계층을 갖는 두드러진 온도의 성층현상이 관찰되었다. FLUTAN Code를 이용한 해석은 속도를 합리적으로 예측할 수 있다는 결과를 보여 주었다.

1. Introduction

The reliable removal of the heat from a core melt located partially at the bottom of a pressure vessel is an important safety criterion. A possible scenario may be that the heat is transferred from the melt to a water filled cavity surrounding the vessel through the wall of the pressure vessel. The cavity water in contact with the pressure vessel is heated and boils with temperature increase and evaporizes. The generated steam is transported to the condensers. The condensed water sinks down in the cavity. Density differences are the driving forces for fluid circulation, i.e., the system is governed by a natural convection flow. These cooling scenarios are studied by using a simple test apparatus with a heated horizontal plate installed in a water filled tank. Although multicomponent flows are more probable in the cavity, present study is focused on natural convection phenomena of the single phase flow in a first step prior to proceeding to the complicated multicomponent flow analysis. The fluid volume below the heated plate and in the plena represents a storage of high heat capacity. The question is how intensively the fluid volume in a tank contributes to the heat transport process. Natural convection below the horizontal heated plate facing downward at high Rayleigh numbers is one of the basic programs in thermal hydraulic phenomena. Aihara *et al.* [1] carried out measurements of velocity and temperature in quasi-two-dimensional buoyancy induced air flow. They measured the local velocities by recording trajectories of fine particles photographically. Faw and Dullforce[2, 3] and Hatfield and Edwards[4] visualized the temperature fields for downward facing plates by using a holographic interferometry and quantified the heat flux. Restrepo and Glicksman[5] measured the local temperature profiles for a square heated and cooled plate in air and evaluated the local heat flux from the measured temperature data. Analytical studies [6−10] were tried to predict natural convection below the downward-facing horizontal heated plate. However the predictions were not successful in all flow parameters mainly because the flow below the heated plate is very unstable and sensitive inherently and similarity methods are not applicable to this problem. In this study, whose parts were presented at the references [11, 12], in order to get a better understaning for the natural convection characteristics in a water tank with a downward-facing horizontal heated plate, the local velocity and temperature are measured by using LDA(Laser Doppler Anemometry) and thermocouples, respectively. This problem can be treated numerically by multidimensional codes able to simulate the

single and two-phase thermal and fluid dynamic processes. The thermal hydraulic FLUTAN computer program[12, 13] is a highly vectorized version of the thermal-hydraulic computer code family COMMIX and represents a tool to analyze the combined fluid dynamics and heat transport for three- dimensional, laminar and turbulent, steady state and transient problems. To access the capability of the FLUTAN code for the simulation of this cooling scenario in a first step, the single-phase thermal and fluid dynamics of the problem is investigated because this procedure provides the basic information for the two-phase flow considerations.

2. Theoretical Background

Typical thermal and fluid flow patterns with a coordinate system for the present test configuration are illustrated schematically in Fig. 1. The governing equations for a two-dimensional natural convection flow are derived by using the Boussinesq assumption without introducing the boundary layer approximation[9, 14].

$$\frac{\partial u}{\partial x}+\frac{\partial v}{\partial y}=0 \tag{1}$$

$$u\frac{\partial u}{\partial x}+v\frac{\partial u}{\partial y}=-\frac{1}{\rho}\frac{\partial p}{\partial x}+\nu\left(\frac{\partial^2 u}{\partial x^2}+\frac{\partial^2 u}{\partial y^2}\right) \tag{2}$$

$$u\frac{\partial v}{\partial x}+v\frac{\partial v}{\partial y}=-\frac{1}{\rho}\frac{\partial p}{\partial y}+\nu\left(\frac{\partial^2 v}{\partial x^2}+\frac{\partial^2 v}{\partial y^2}\right)+g\beta(T-T_\infty) \tag{3}$$

$$u\frac{\partial T}{\partial x}+v\frac{\partial T}{\partial y}=\alpha\left(\frac{\partial^2 T}{\partial x^2}+\frac{\partial^2 T}{\partial y^2}\right) \tag{4}$$

where ν, g, β and α are kinematic viscosity, gravitational acceleration, thermal expansion coefficient and thermal diffusivity, respectively. There are two kinds of natural convection flow in this test configuration, i.e., horizontal flow below the heated plate and vertical flow in the plenum. In the horizontal flow region, the flow is governed dominantly by the u-momentum equation (2). Introducing the boundary approximation below the heated plate, equation (3) yields

$$\frac{\partial p}{\partial y}=\rho g\beta(T-T_\infty) \tag{5}$$

Hence the buoyancy force of last term in equation(3) influnces the horizontal velocity indirectly by way of the hydrostatic pressure difference. The pressure difference is the direct driving force. Since, in stationary flow, hydrostatic pressure distribution depends only on the local temperature distribution in the boundary layer, the pressure is higher in the hot fluid beneath the plate than in the cold fluid at the same depth.

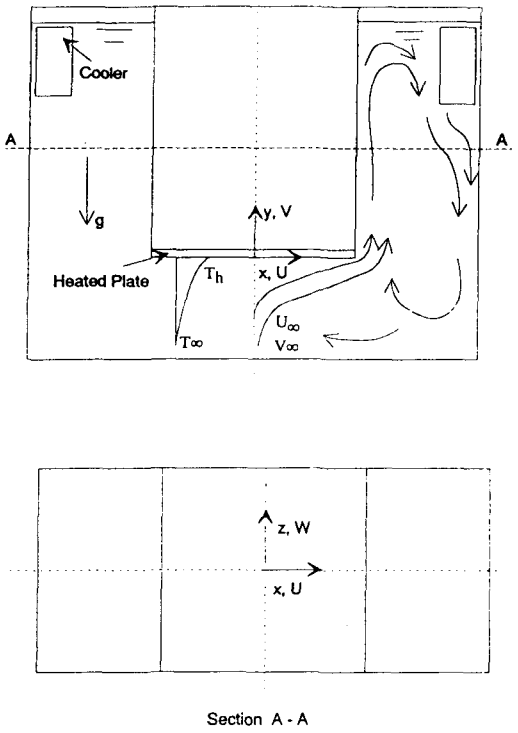

Fig. 1. Typical Thermal and Fluid Flow Pattern in a Water Tank with a Heated Plate and Coordinate System

This pressure difference forces the fluid horizontally outward. In the plenum of the vertical velocity dominated-flow region, the flow is governed by the v-momentum equation(3). The buoyancy force which is the major force due to density difference drives the flow upward near inner wall and downward near the outer tank wall. In order to analyze the whole flow area, governing equations (1)−(4) mentioned above should be considered without boundary layer approximation.

3. Test Facility

The test facility is schematically represented in Fig. 2 together with its main dimensions in millimeters. The pressure vessel is simulated by an insulated box with a height of 300mm and a square cross section of 150×150 mm. The heat source is modeled by a heated plate(150×150×15 mm) horizontally mounted at the bottom of the box. The heated plate is a square copper plate which has long holes for inserting heating lines and thermocouples. The box with heated plate symmetrically installed in an open-topped water filled glass tank. This installation realizes a U-type water volume with two elbow type plena of identical dimensions on both sides of the box. Each plenum is equipped with a two-sided plate-type cooler (150×12×105 mm) immersed in the water. The primary flow along the cooling surfaces of the cooler is guided by two plexiglass plates vertically positioned 3. 6mm from either side of the cooler. The coolers are installed symmetrically to the box at identical elev ations to the heated plate. The thickness(H) of the water layer between the heated plate and the bottom wall of the tank can be easily varied by placing a filling body of appropriate dimension at the bottom of the tank. The tank, the body and the filling bodies are made of glass and plexiglass to allow a visualization of the flow. At the surface, the whole facility is covered with heat insulation during all experiments. The window for the LDA measurements is reduced to a minimum to minimize heat losses to the environment. The experimental parameters are the heater power and the water layer thickness between heated plate and tank bottom. Velocity and temperature measurements were performed with varying the water layer thickness, H, below the heated plate, i.e., H=10, 40, and 90 mm. Two levels of heat power for each height, P=217W and 438W were tested. During all experiments, the distance between heated plate and water surface was kept constant(275 mm). Hence the total water volume varied, for the various water layer thickness H. The whole circulating flow phenomena are two-dimensional except region (about 5mm from front and back window wall, which was confirmed by flow visualization.

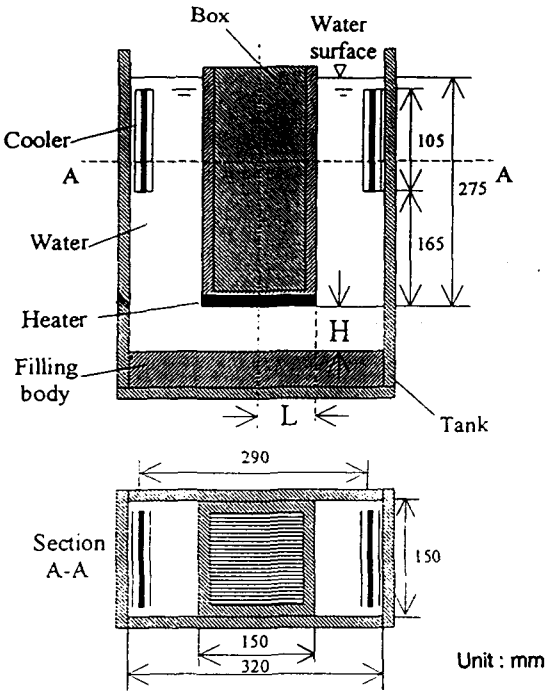

Fig. 2. Geometry of the Test Facility

4. Instrumentation and Test Procedure

Velocity measurements are performed by varying

the distance from the edge of the heated plate, y=65(V1), 85(V2), 105(V3), 125(V4), 145(V5), 155 (V6), and 225mm(V7) and the distance from the center of the heated plate, which are illustrated in Figs. 3 and 4. All measurements were performed at z=0 mm. Velocity components in main directions, i.e., parallel to the side wall (vertical velocity component in measuring direction 1) and the heated plate (horizontal velocity component in measuring direction 2) were measured. Local velocities are measured using a one-component DISA 55X Fiber Optic Laser Doppler Anemometry(FOLDA) aligned with the backward scatterred mode. The probe head is positioned outside the test facility and is connected to a PC controlled 2D traversing system. Local fluid temperatures are measured by using NiCr-Ni thermocouples of 0. 25mm outer diameter along the measuring direction as shown in Fig. 3. Before the start of the experiments, all measuring devices were calibrated. The following uncertainties can be assumed:

- flow velocities 〈 ≥ 0.5 mm/s
- temperatures 〈 ≥ 0.1°C
- core power 〈 ≥ 2%
- heat losses 〈 ≥ 4%

The preliminary measurements of the heated plate were performed from the some thermocouples embedded in the central and outer region of the heated plate. Deviation from the average temperature is within 1%. Basing on this fact that the isothermal condition was almost satisfied, the heated plate temperature was obtained at central region of the heated plate. After installation and calibration of all measuring devices, the heat power is switched on and the coolers are put in operation. At the secondary side of each cooler, the circulating volume flow rate of 0. 0163 ℓ /s and inlet temperature 10°C are kept constant during the course of the experiment independent of the core power. When the steady state flow conditions are reached, velocity and temperature are

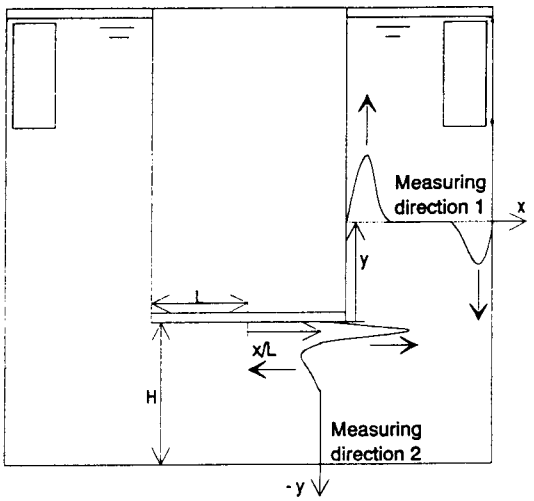

Fig. 3. Measuring Positions and Directions Showing Typical Velocity Profiles

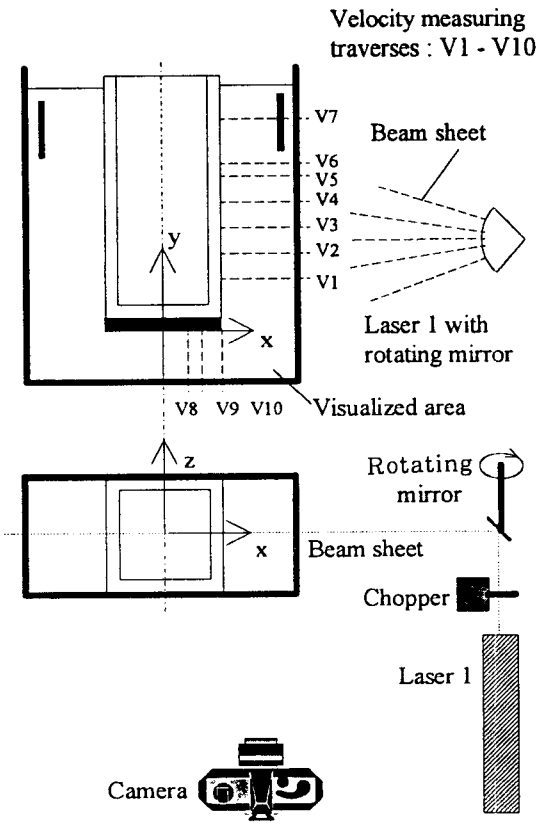

Fig. 4. Measuring Traverses and Flow Visualization Method

measured by using a LDA and movable thermocouples, respectively. The matrix of the experimental cases is given in Table 1. For the main parameters, namely the water layer thickness H and the heat power P are indicated. As for the characteristic number of natural convection flow, when Rayleigh number is defined as Ra =Gr Pr with the Grashof number: $Gr = g\beta(T_h - T_\infty) L^3/\nu^2$, and the Prandtl number: $Pr = \nu/\alpha$, where T_h, T_∞ and L indicate the measured temperature at the center of the heated plate, the water temperature near the bottom of the tank, and the characteristic length of one-half of the heated plate width, respectively, the range of the Ra number is obtained from 1.41×10^8 to 9.5×10^8. The flow fields are visualized by using the method illustrated in Fig. 4. A laser beam of 1 mm diameter is directed to a rotating mirror. The produced beam sheet visualized particles (Plyolite, 1.04 g/cm^3) equally distributed in the water. A beam chopper allows to interrupt the laser beam to quantify the velocity and flow direction of the particles recorded photographically.

5. Computer Code Simulation

A highly vectorized version of the thermal-hydraulic computer code FLUTAN[12, 13] has been used for the numerical prediction of the experiments. The slab geometry is modeled by a 3D noding scheme with about 3000 volume cells. The following boundary conditions are specified: Constant heat flux normal to the heated wall surfaces are assumed. At the coolers secondary side, the heat transfer is determined on the basis of the measured mass flow rate and inlet temperature. At the primary side, boundary conditions account for fluid convection, thermal capacity of the walls, and heat transfer to the surround-

Table 1. Matrix of Measurements

Height between heated plate and bottom wall, H (mm)	Heater Power, P (W)	Measuring positions			
		Measuring direction 1, y (mm)		Measuring direction 2, x/L	
		Velocity	Temperaure	Velocity	Temperaure
10	217	65, 105, 145		0.47, 0.67 1.00	
	438	65, 105, 145		0.47, 0.67 1.00	
40	217	65, 105, 145	65, 105, 145	0.47, 0.67 1.00	0.0, 0.33, 0.53, 1.0
	438	65, 105, 145	65, 105, 145	0.47, 0.67 1.00	0.0, 0.33, 0.53, 1.0
90	217	65, 105, 145	65, 105, 145	0.47, 0.67 1.00	0.0, 0.1, 0.2, 0.33, 0.53, 0.8, 1.0
	438	65, 85, 105, 125, 145, 155, 225	65, 105, 145	0.47, 0.67 1.00	0.0, 0.1, 0.2, 0.33, 0.53, 0.8, 1.0

ing water. All computations are based on laminar flow conditions.

6. Results and Discussions

6.1. Velocity Profiles

Fig. 5 shows the vertical velocities along horizontal traverses V1 to V7 for a power of 438W and a water layer thickness of H=90mm. The measurements at powers of 217W taken along traverses V1, V3, and V5 are also included in the graph. For the water thickness of H=40 mm, the measured velocities along traverses V1, V3, and V5 are represented in Fig. 6 at powers of 217 and 438 W. In all cases maximum velocities occur near the wall of the box, where hot water rises upward. The negative velocities occur near the wall of the tank where cold water coming from the coolers flows downward. Between these areas of fast flowing fluid, a large region with nearly stagnant fluid is observed. This behavior is measured for different powers. The maxima of the upward or downward velocities, however, are increased by about 50% with doubling the power. With increasing the y-position of the measuring traverses a more and more pronounced shear flow phenomena taking place near the inner wall can be detected. This is indica ted by the measured negative vertical velocities in the range of 5−10 mm distance from the inner wall. This result implies that a small circulation exists in this region in opposite direction of the large circulation in the whole flow area. Downward flow below the coolers is not shown at y=225 mm(V7), since this measuring traverse is located above the lower edge of the coolers. Along the V6(y=155 mm) measuring traverse which is about 10 mm below the cooler the velocities of the downward fluid flows from the cooler. With increasing distance from the cooler(decreasing y-position), the maximum values are more and more deflecteted to the outer tank wall and increase due to flow acceleration. This is a kind of Coandar effect caused by depressurization in the gap

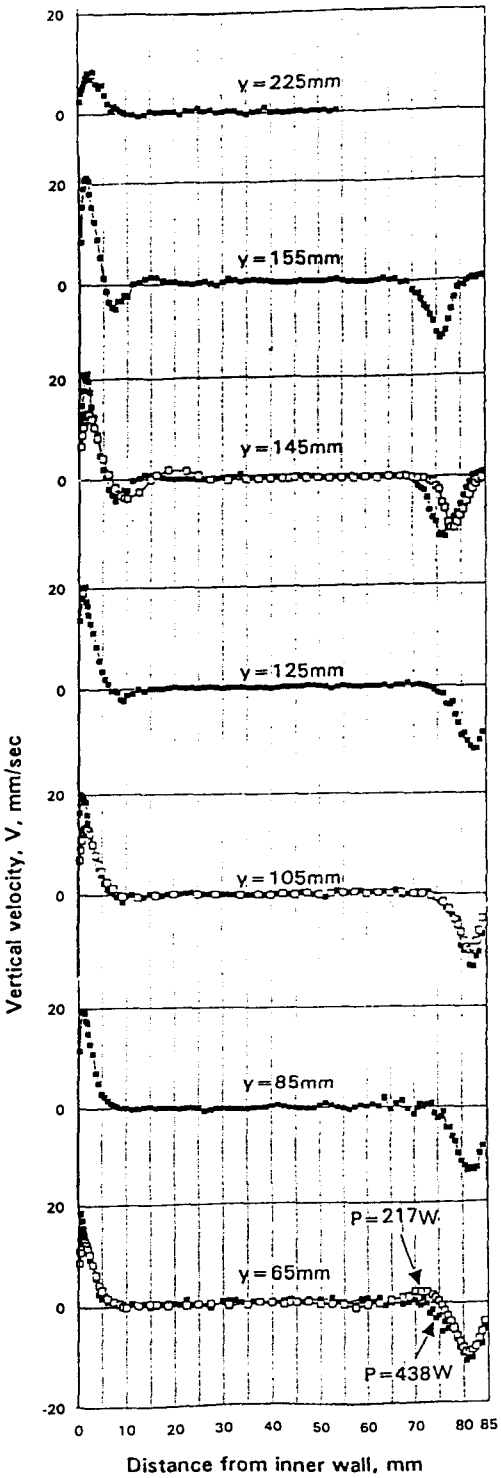

Fig. 5. Developing Vertical Velocity Profiles in the Plenum for H=90 mm

between the downward flowing water and the tank wall. The lower measuring traverse indicates a reduction of the maximum downward velocity. In the region near the heated plate this flow is already influenced by the flow within the water layer thickness below the heated plate. Figs. 7 and 8 show the velocities along the traverses V1 and V3 for 217W and different water layers. It is observed that the thickness of the water layer below the heated plate seems to be of no decisive influence on the local flow in the plenum region above the heated plate. The horizontal velocities measured along the vertical traverses V8(x/L=0.47), V9(x/L=0.67), and V10(x/L=1.0) below the heated plate are indicated in Figs. 9 and 10. Fig. 9 shows the horizontal velocities for the water layer thickness of H=90 mm and different powers. And Fig. 10 represents the effect of the water layer thickness on the horizontal velocities. In general, all data show that the highest velocities are measured near the heated surface. The higher the power is, the higher the maximum velocities are. The boundary layer is in a very thin fluid layer with a thickness of < 5 mm. With increasing x/L the thickness of the boundary layer is reduced. Near the heated surface the velocities increase with the lateral distance from the cen-

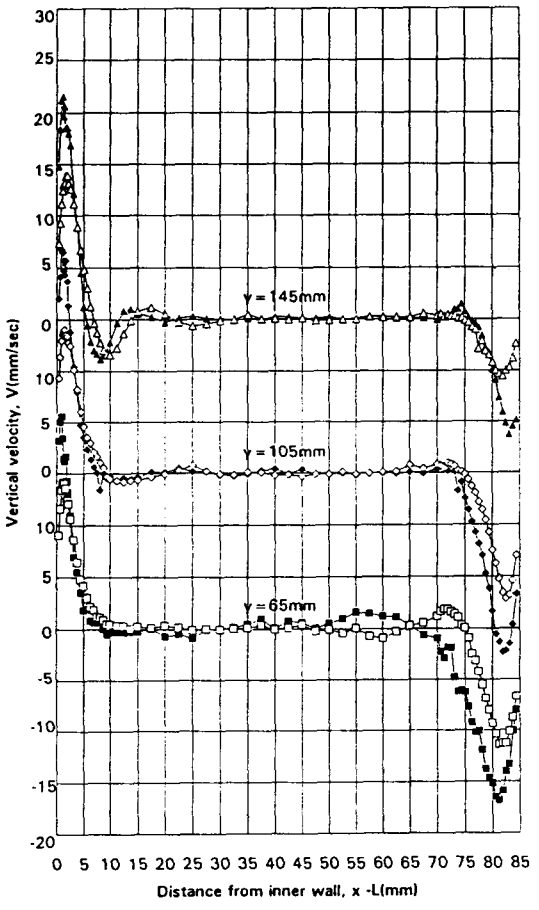

Fig. 6. Vertical Velocity Profiles for H=40 mm and Different Powers (Black symbol: P=438 W, White symbol: P=217 W)

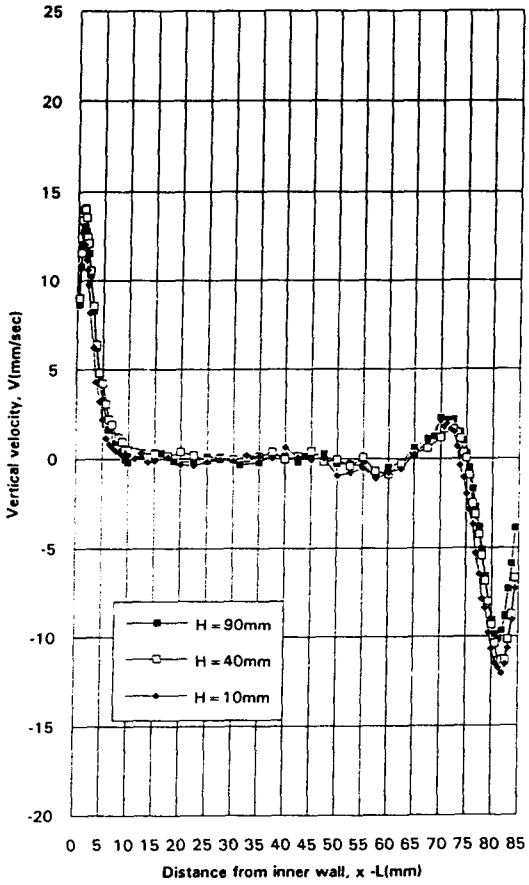

Fig. 7. Vertical Velocity Profiles at y=65 mm, P=217 W and Different Heights, H

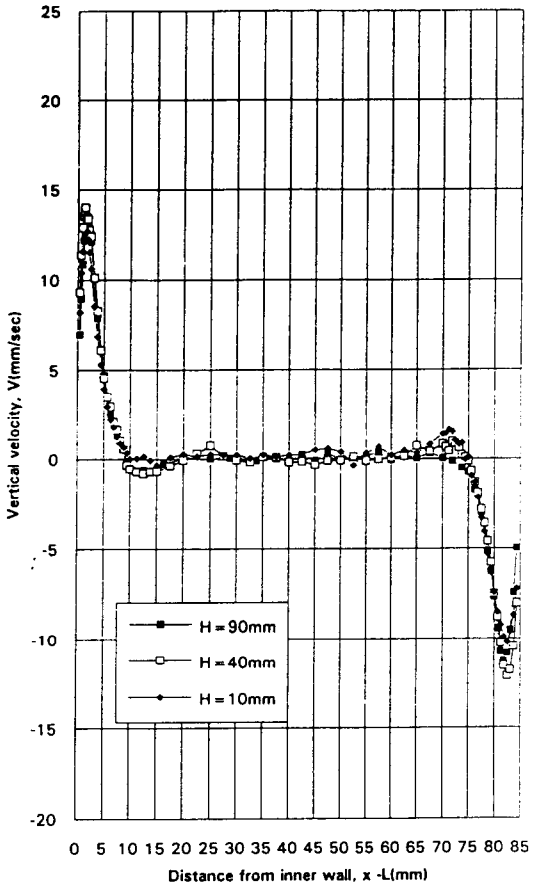

Fig. 8. Vertical Velocity Profiles at y=105 mm, P=217 W and Different Heights, H

ter of the heated plate and with the heated power. The maximum value of the velocity below the heated plate is measured at the measuring location, 0. With increasing distance from the heated plate(decreasing y) the flow direction is reversed and fluid flows inward. In the case of H=90 mm, the reversed flow region is from y=−5 mm to −30 mm. It seems that below this region the flow is rather stagnant. For H=40 mm, the reversed flow region is not so pronounced. The nearly stagnant flow region starts from y=−20 mm. In the case of H=10 mm, the flow is reversed ranging from y=−2.5 mm to the bottom.

6.2. Temperature Profiles

Temperature profiles at steady state are measured by movable thermocouples at measuring directions 1 and 2 indicated in Fig. 3. Temperature data below the heated plate for H=90mm and heat power, 438W, are shown in Fig. 11. It is observed from the data that thermal boundary thickness is very thin less than 5mm. At the remote region from the plate, the temperatures are nearly constant, which implies that the flow region is stratified thermally with the thermal

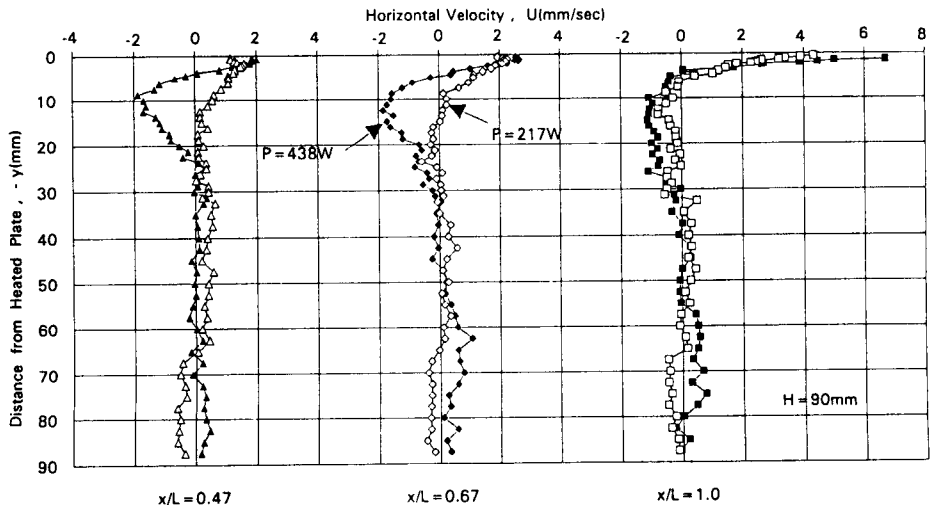

Fig. 9. Horizontal Velocities below the Heated Plate for P=438 W and Different Heights, H

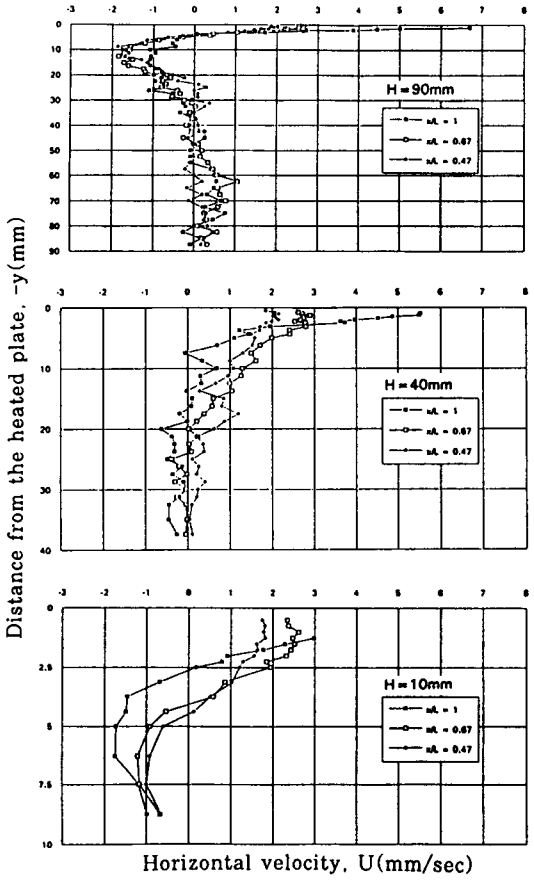

Fig. 10. Horizontal Velocities below the Heated Plate for P=438 W and Different Heights, H

boundary. With increasing x/L, temperature gradients below the plate become higher, which means the higher local heat transfer rates. The higher heat transfer rates in outer region of the plate are due to the higher velocities, of which results were discussed previously. Fig. 12 shows the temperature profiles in the plenum above the plate. The results represent that the hot fluid flows upward near inner wall and the cold fluid flows downward from the cooler. The cold fluid is mixed with neighboring fluid in the lower region of the plenum. A circulation in downward flow direction at 5 mm away from the inner can be detected from the temperature results at that region. Local Nusselt numbers below heated plate were evaluated from measured temperature data. Local Nusselt number, Nu, is defined by

$$Nu=\frac{q_w L}{x(T_h-T_\infty)} \tag{6}$$

where q_w is local surface heat flux, and estimated from the temperature gradient at the heated plate surface. Local Nusselt numbers devided by the $Ra^{0.2}$ are plotted and compared with Aihara et al. [1] and Singh *et al.* [15, 16] in Fig. 13. The results show same trends with the others' data. Fig. 14 shows a comparison of the average Nusselt number, $\overline{Nu}$, along the heated plate with data by the others[6, 7], where $\overline{Nu}$ is defined by

$$\overline{Nu}=\frac{1}{L}\int_0^L \frac{q_w}{x(T_h-T_\infty)}\,dx \tag{7}$$

It is generally noted that the present results are distributed within the range of these two correlations, $\overline{Nu}=0.25\ Ra^{0.25}$ in Ref. 6 and $\overline{Nu}=0.44\ Ra^{0.2}$ in Ref. 7. More comparisons of the average Nusselt numbers with the others are listed in Table 2. It is observed that present results are not much scattered from the others' data.

6.3. Flow Visualization

The flow fields are visualized by taking pictures of the illuminated area indicated in Fig. 4. A visualized flow photograpy below the plate for H=90mm and power, 217W is represented in Fig. 15. It is observed that the fluids below the plate are directed to outward and turning around the plate edge. The flow in the plenum for H=90 mm and power 217W is visualizd photographically as shown in Fig. 16. It can be seen from this picture that the flow circulates largely in whole flow region and some vortexes at the higher region near inner wall and in the lower plenum region can be observed. The features of the flow visualization results coincide with those of the velocity and temperature.

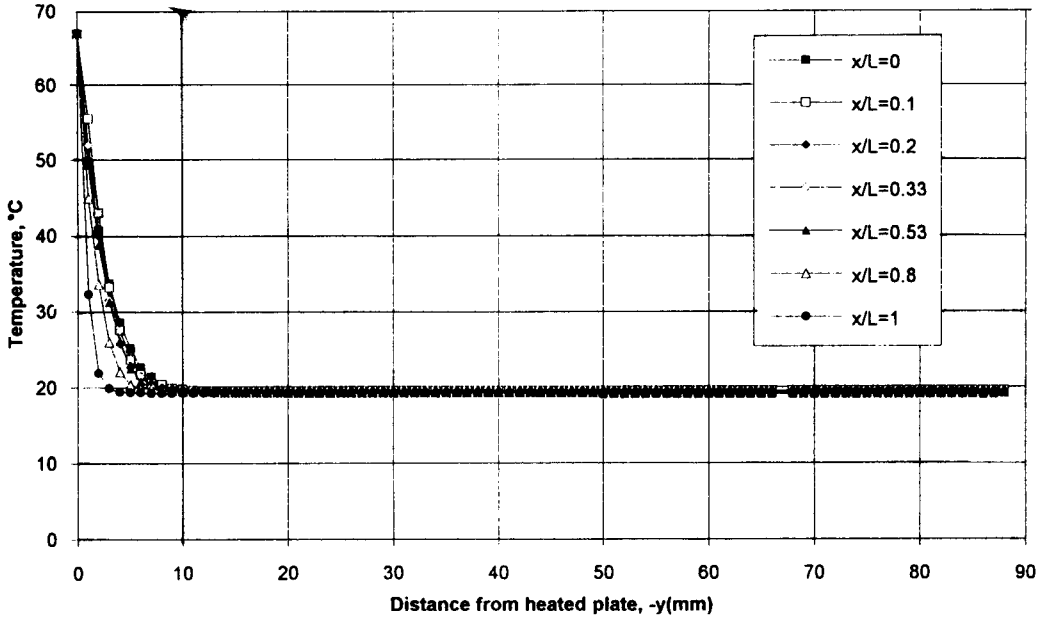

Fig. 11. Temperature Profiles below the Peated Plate for H=90 mm and P=438 W

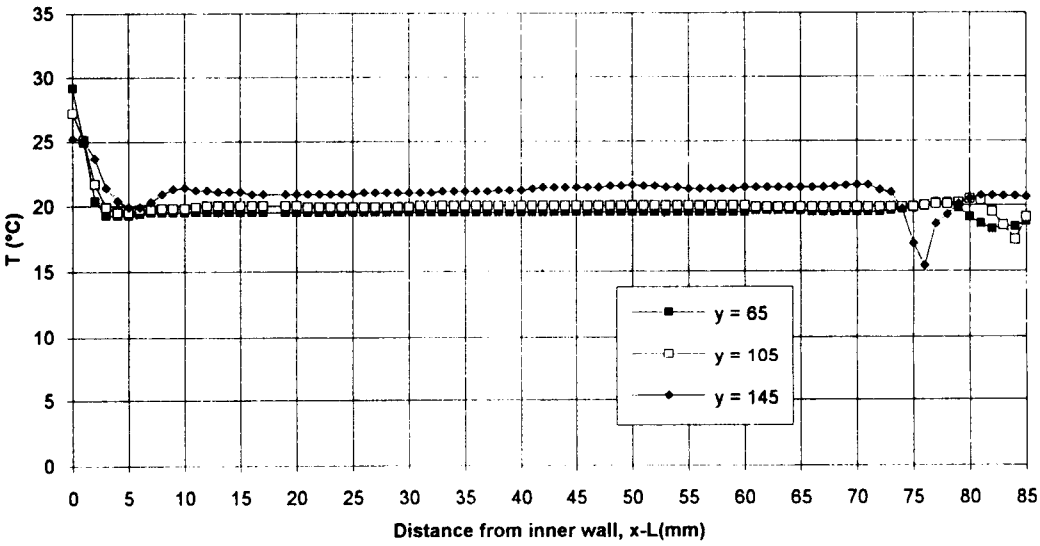

Fig. 12. Temperature Profiles in the Plenum for H=90 mm and P=438 W

6.4. Comparison of Measured and Computed Velocities

Velocity fields were visualized. The velocities and directions of the particles can be demonstrated by pulsed illumination varying the pulse frequency. This method is used to determine the flow fields in the model. The visualized flow fields are compared with

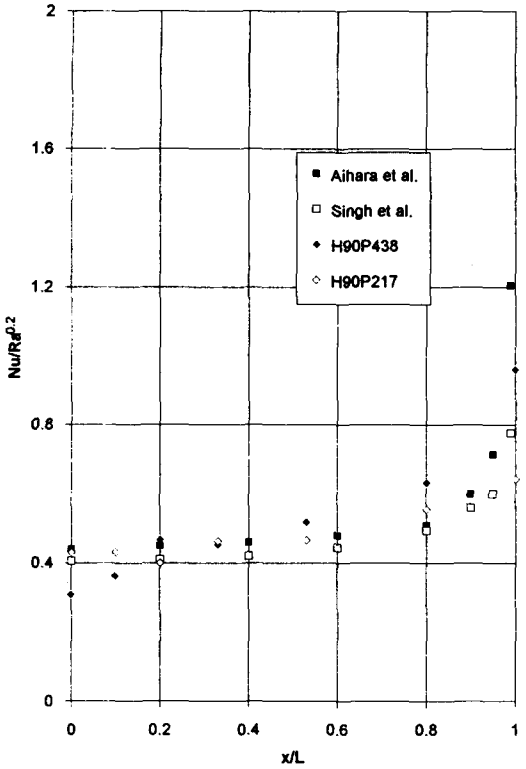

Fig. 13. Local Nusselt Numbers with the Others(Aihara et al. [1], Singh et al. [15, 16], Present Data: H90P438(H=90 mm, P=438W), H90P217 (H=90 mm, P=217 W))

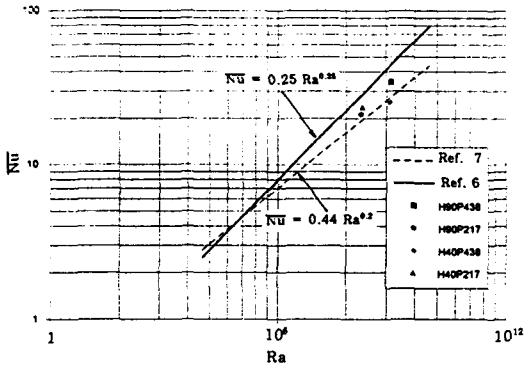

Fig. 14. Average Nusselt Numbers with the Others(Clifton and Chapman[7], Chapman[6], Present Data: H90438W(H=90 mm, P=438 W), H90P217(H=90 mm, P=217 W), H40P438(H=40 mm, P=438 W), H40P217(H=40 mm, P=217 W))

computed velocity vector fields as shown in Fig. 17. The photo on the left hand side is taken during the heat-up phase, 1200s after start of the heating. The photo on the right hand side is typical for steady stat e conditions at about 8000s. In both cases the power is 438W, the thickness of the water layer below the heated plate is H=90 mm. Each photo represents an illumination time of 16s. A strong upward flow

Table 2. Comparison of Average Nusselt Number $\overline{Nu}$ for the Heated Downward-Facing Plate

Authors	$\overline{Nu}/Ra^{0.2}$	Remarks
Present work		Experimental two-dimensional flow, square plate, in water
	0.548	H=90 mm, P=438 W, Ra=9.5×10^8
	0.49	H=90 mm, P=217 W, Ra=1.41×10^8
	0.41	H=40 mm, P=438 W, Ra=8.9×10^8
	0.536	H=40 mm, P=217 W, Ra=1.66×10^8
Aihara *et al.* [1]		Experimental quasi-two-dimensional flow, in air
	0.509	Ra=1.02×10^6
	0.500	Ra=7.16×10^6
Sounders *et al.* [17]		Experiment, rectangular plate, in air
	0.523	Ra=9.4×10^6
	0.526	Ra=6.61×10^6
Birkebak *et al.* [18]	0.681	Experiment, square plate, in water
Singh *et al.* [15, 16]	0.46	Theory, two-dimensional flow, Pr=0.7

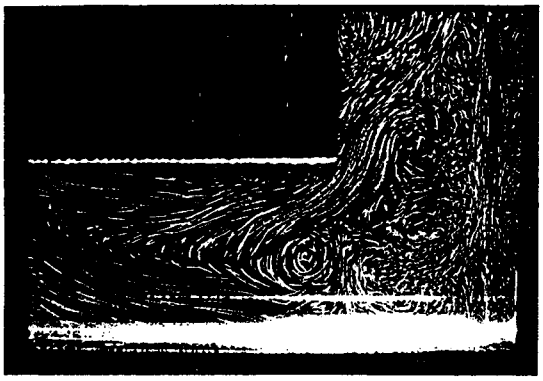

Fig. 15. Visualized Velocity Fields below the Heated Plate for H=90 mm and P=217 W

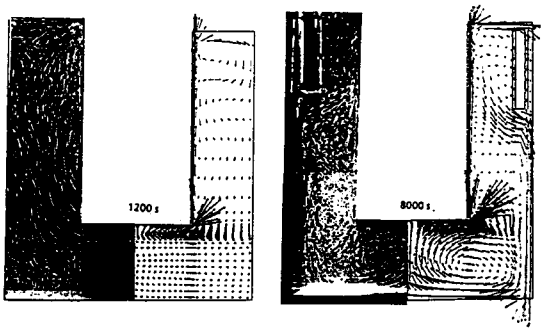

Fig. 17. Comparison of Computed and Visualized Velocity Fields during Heat-Up Phase(1200s) and for Steady State Conditions (8000s)

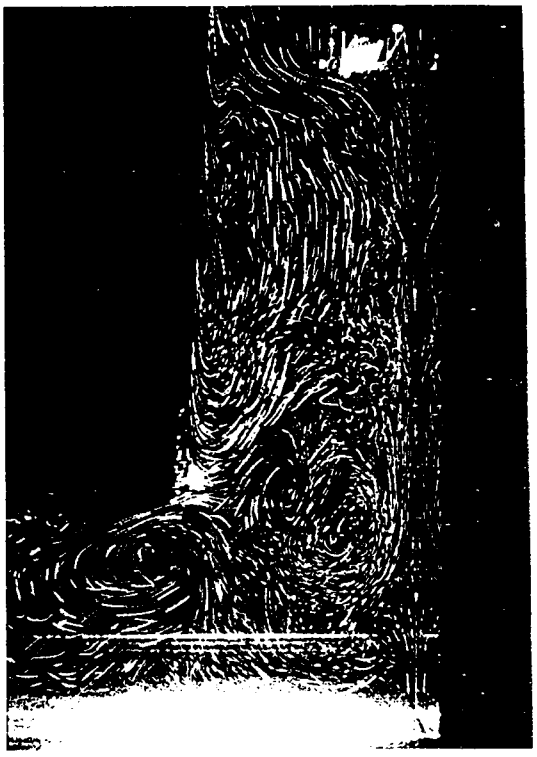

Fig. 16. Visualized Velocity Fields in the Plenum for H=90 mm and P=217 W

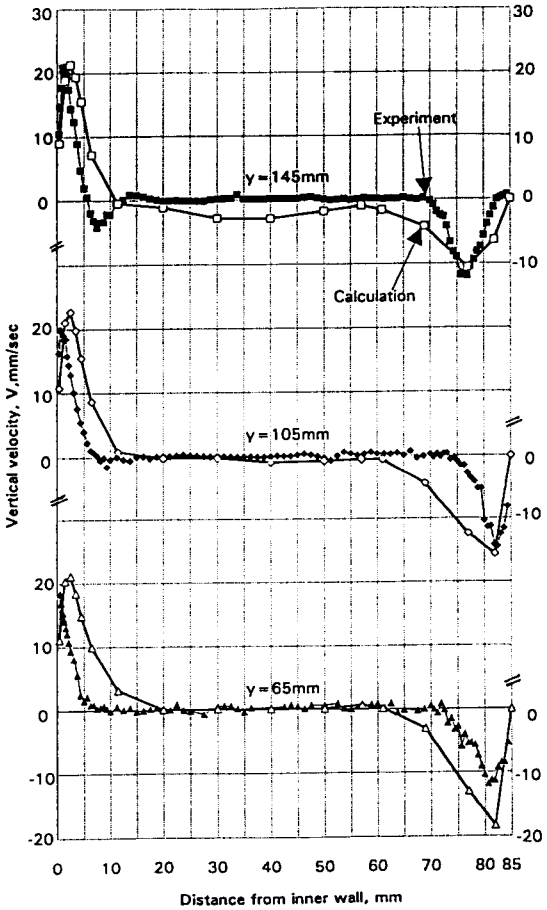

Fig. 18. Comparison of Measured and Calculated Velocities along Traverses Y=65, 105, 145 mm for H=90 mm. P=438 W

can be detected near the box wall initiating a vortex near the free water surface. In a large portion of the area below the heated plate, the flow is rather stagnant. In the graph on the right hand side, this stagnant flow area is no longer visible. A large vortex can also be seen in the photo. The rotational center, however, seems to be shifted toward the tank wall. In addition a second vortex is formed right below the heated plate. A comparison of computational and test data is shown in Fig. 18 for the vertical velocity profiles along traverses V2, V3 and V4. The power is 438W and H=90 mm. As can be seen the measured vertical velocities indicate a maximum near the tank wall and these values correspond to the measurements. But the thickness of the upward and downward flowing fluid is too large in the circulations. Therefore, the circulating mass flow from the calculations is about 50% higher than indicated in the measurements. This leads to a smaller temperature difference along the water plenum under steady state conditions.

Additional investigations are necessary to clarify this local discrepancy which is mainly a result of the coarse nodalization of the plenum. In general, however, it can be stated that the stream line photography and the computations are qualitatively in agreement.

7. Summary and Conclusions

Experimental and computational studies were carried out using a simple setup with a horizontal heat source which is movable in axial direction within a water filled tank. Fluid temperatures and velocities were measured under different buoyancy-driven operational conditions. Following a tran- sient heat-up phase, coolers are put into operation to reach steady-state values where the heat input was equal to the heat removal. For identical boundary conditions, the heat power and the water layer below the heated surface were varied.

It was observed from measured velocity and temperature data and flow visualizations that a very effective flow circulation starts right after the start of the heating. During the heat up phase, the hot fluid flows upward intensively within a small water layer at the box wall. The cool water from the coolers sinks toward the bottom of the tank. This flow initiates a flow circulation in the whole water volume stored in the plenum above the heated plate. The flow for the higher power of the heated plate circulates more intensively than the lower power flow.

Below the heated plate, only a thin boundary less than 5 mm is involved in the heat transport process. In the case of thick water layers, hence, a large portion of water is nearly stagnant and a remarkable temperature stratification can be observed with very thin thermal boundary. The whole heat transport process is not influenced significantly by the water layer thickness below heated plate but mainly by the water volume above the heated plate.

Numerical predictions using the FLUTAN code were compared with the experimental data. Over wide range of parameters, the comparison shows a qualitative agreement for the data available up to now. Additional calculations are in progress to clarify the unsolved problems.

Nomenclature

g	graviational acceleration , m/s^2
Gr	Grashof number, $g\beta(Th - T_\infty)L^3/\nu^2$
H	height between heated plate and bottom wall, m
L	half-width of the heated plate, m
Nu	local Nusselt number, $q_w L/(\lambda(T_h - T_\infty))$
$\overline{Nu}$	average Nusselt number
P	heater power, W
p	pressure, Pa
Pr	Prandtl number, ν/α
q_w	local surface heat flux, W/m^2
Ra	Rayleigh number, Gr Pr

T	temperature, °C
T_h	heated plate temperature, °C
T_∞	temperature at a remote region below heated plate, °C
u, v, w	velocity components, m/sec
U_∞, V_∞	velocities at a remote region below heated plate, m/sec
x, y, z	coordinate system, m

Greek symbols

α	thermal diffusivity	m^2/s
β	thermal expansion coefficient	$°C^{-1}$
χ	thermal conductivty	W/(m. °C)
ν	kinematic viscosity	m^2/s
ρ	density	kg/m^3

References

1. T. Aihara, Y. Yamada and S. Endo, "Free convection along the downward-facing surface of a heated horizontal plate," Int. J. Heat Mass Transfer, Vol. 15, pp. 2535−2549, 1972.
2. R.E. Faw and T.A. Dullforce, "Holographic interferometry measurement of convective heat transport beneath a heated horizontal plate in air," Int. J. Heat and Mass Transfer, Vol. 24, No. 5, pp. 859−869, 1981.
3. R.E. Faw and T.A. Dullforce, "Holographic interferometry measurement of convective heat transport beneath a heated horizontal circular plate in air," Int. J. Heat and Mass Transfer, Vol. 25, No. 8, pp. 1157−1166, 1982.
4. D.W. Hatfield and D.K. Edwards, "Edge and aspect ratio effects on natural convection from the horizontal heated plate facing downward," Int. J. Heat Mass Transfer, Vol. 24, No. 6, pp. 1019−1024, 1981.
5. F. Restrepo and L.R. Glicksman, "The effect of edge conditions on natural convection from a horizontal plate," Int. J. Heat Mass Transfer, Vol. 17, pp. 135−1452, 1974.
6. A.J. Chapman, Heat transfer, 2nd edn., Macmillan, New York 1967.
7. J.Y. Clifton and A.J. Chapman, "Natural convection on a finite size horizontal plate," Int. J. Heat Mass Transfer, Vol. 12, pp. 1573−1584, 1969.
8. T. Fujii, H. Honda and I. Morioka, "A theoretical study of natural convection heat transfer from downward-facing horizontal surfaces with uniform heat flux," Int. J. Heat Mass Transfer, Vol. 16, pp. 611−627, 1973.
9. T. Schulenberg, "Natural Convection Heat Transfer below Down-ward Facing Horizontal Surfaces," Int. J. Heat Mass Transfer, Vol. 28, No. 2, pp. 467−477, 1985.
10. F.J. Higuera, "Natural Convection below Heated Horizontal Rectangular Plates," Int. J. Heat Mass Transfer, Vol. 36, No. 14, pp. 3565-3571, 1993.
11. S.K. Yang, M.K. Chung and H. Hoffmann,"Experimental study on natural convection in a water tank with a horizontal heated plate facing downward," Proceeding of the Korea Nuclear Society Spring Meeting, Pohang, Korea, pp. 385−390, 1994.
12. H. Hoffmann, S.K. Yang, R. Kapulla, D. Weinberg and K. Dres, "Investigations into the transient natural convection in a tank with horizontally arranged heater plate," Proceedings of Conference on New Trends in Nuclear System Thermohydrauics, Pisa, Italy, pp. 575−583, 1994.
13. H. Borgwaldt, W. Baumann and G. Willerding, "FLUTAN input specifications-KfK 5010,"Kernforschungszentrum Karlsruhe, Germany.
14. E.R.G. Eckert and R.M. Drake, JR., Analysis of heat and mass transfer, McRraw Hill, 1972.
15. S.N. Singh, R.C. Birkebak and R.M. Drake, JR., "Laminar free convection heat transfer from downward-facing horizontal surfaces of finite dimensions," Progress in Heat and Mass Transfer, Vol. 2, pp. 87, Pergamon Press, Oxford, 1969.
16. S.N. Singh and R.C. Birkebak, "Laminar free convection from a horizontal finite strip facing downwards," ZAMP 20, pp. 454−461, 1969.

17. O.A. Saunders, M. Fishenden and H.D. Mansion, "Some measurements of convection by an optical method," Engineering, pp. 483−485, May 1935.

18. R.C. Birkebak and A. Abdulkadir, "Heat transfer by natural convection from the lower side of finite horizontal heated surface," Preprints 4th Int. Heat Transfer Conf., Paris 4 NC 2. 2 1970.